

Thermal Stability Analysis of Polyurethane Foams Made from Microwave Liquefaction Bio-Polyols with and Without Solid Residue

Xing-Yan Huang,^{a,b,*} Cornelis F. de Hoop,^{a,*} Xiao-Peng Peng,^{c,d} Jiu-Long Xie,^b Jin-Qiu Qi,^b Yong-Ze Jiang,^b Hui Xiao,^b and Shuang-Xi Nie^d

The thermal stabilities of bio-based polyurethane (PU) foams made from liquefaction bio-polyols with and without solid residue were analyzed by thermogravimetric analysis (TGA) and Fourier transform infrared spectrometry (FTIR). Yaupon holly (*Ilex vomitoria*) was subjected to microwave liquefaction at different reaction temperatures to characterize the variations of bio-polyol and solid residue with temperature. The results indicated that the solid residue decreased when the temperature increased from 120 °C to 160 °C, while it increased slightly when further increasing temperature to 200 °C. The hydroxyl number decreased with increased reaction temperature. The TGA of PU foams demonstrated that the use of liquefaction bio-polyol with and without solid residue to produce PU foam increased the thermal stability of biofoams as compared with petro-based foam. Moreover, the presence of solid residue in bio-polyol enhanced the thermal stability of biofoams. The FTIR analysis of PU foams suggested that the solid residue had a negative effect on the formation of urethane bonds.

Keywords: Thermal stability; Polyurethane foam; Liquefaction; Microwave liquefaction; Solid residue

Contact information: a: School of Renewable Natural Resources, Louisiana State University Agricultural Center, Baton Rouge, LA 70803, USA; b: College of Forestry, Sichuan Agricultural University, Chengdu, Sichuan 611130, P. R. China; c: State Key Laboratory of Tree Genetics and Breeding, Research Institute of Forestry, Chinese Academy of Forestry, Beijing 100091, P. R. China; d: Guangxi Key Laboratory of Clean Pulp & Papermaking and Pollution Control, Nanning, Guangxi 530004, P. R. China;

* Corresponding authors: xhuan19@lsu.edu; cdehoop@lsu.edu

INTRODUCTION

Rigid polyurethane (PU) foam is one of the most important polymeric materials due to its versatile properties, such as low density, low thermal conductivity, and high strength. It has been widely used in various applications including packaging, construction, insulation, and transportation. However, the PU foam industry is still highly dependent on petro-based chemicals due to its two major feedstocks, polyol and isocyanate. With growing concern for environmental protection and the rapid depletion of fossil fuels, numerous efforts have focused on the substitution of petro-based polyols with bio-based polyols, such as vegetable oil (Zhang and Kessler 2015), and bio-polyol derived from lignocellulosic biomass (Liang *et al.* 2006; Kumar *et al.* 2015). It has been demonstrated that the PU foams made from bio-polyol are comparable to petro-based ones (Gama *et al.* 2015).

As a promising route to convert lignocellulosic biomass into useful bio-polyol, the liquefaction process could break down the main chemical components (*i.e.*, hemicellulose, lignin, and cellulose) to produce hydroxyl-rich liquefaction products (Liu *et al.* 2011;

Zhang *et al.* 2012; Cheumani-Yona *et al.* 2014), including liquid bio-polyol and solid residue. In general, liquefaction products with and without solid residue can be used for producing PU foams (Esteves *et al.* 2017). From a cost-saving viewpoint, it is better to directly use the liquefaction products without removing solid residue because it saves a separation process. Currently, a considerable amount of biomass has been liquefied to prepare bio-based PU foams, such as wheat straw (Chen and Lu 2009), cornstalk (Yan *et al.* 2008), sugar cane bagasse (Hakim *et al.* 2011), waste paper (Lee *et al.* 2002), rape straw (Huang *et al.* 2018), wood (Cheumani-Yona *et al.* 2014), and lignin (Xue *et al.* 2015).

One of the most important applications of PU foams is in thermal insulation, so their thermal behaviors are very important. The primary thermal decomposition of PU foams is the degradation of urethane bonds starting to dissociate at approximately 150 °C (Zhang *et al.* 2013). The degradation of urethane bonds leads to the formation of primary amines, secondary amines, and carbon dioxide (Hablot *et al.* 2008). Considering that the thermal stability of PU foam is closely related to the isocyanate index (Zhao *et al.* 2012) and the chemical structures of PU foam (Zhang *et al.* 2013), it is necessary to characterize the production of PU foam using thermogravimetry. Fourier transform infrared spectroscopy (FTIR) analysis has been demonstrated as an effective way to characterize the production of PU foam (Tien and Wei 2001; Ebert *et al.* 2005; Zhang *et al.* 2013). Additionally, the thermal behaviors of biofoams made from liquefaction bio-polyols with solid residue in a nitrogen and air atmosphere have been reported in previous work (Yan *et al.* 2008), but the influence of solid residue on the chemical structure of PU foam remains unclear.

Yaupon holly (*Ilex vomitoria*) is one of the most widespread woody underbrush species in the southeastern United States, and it could undermine the forest health and safety due to its biofuel-like nature during catastrophic wildfires. The removal and utilization of woody underbrush could reduce forest fuel loading levels and improve overall forest health. The hydrogen bonding index (HBI) of carbonyl in urethane bonds and ether index (EI), corresponding to the soft and hard segments in PU foams, respectively, were determined from FTIR spectra to analyze the differences in chemical structure between the biofoams made from bio-polyol with and without solid residue. The objective of this study was to investigate the thermal stability of bio-based PU foam made from liquefaction bio-polyols with and without solid residue. Therefore, Yaupon holly was liquefied at different reaction temperatures in the range of 120 °C to 200 °C, because it could produce entirely different solid residues under microwave irradiation. The final objective was to commercialize the PU foam from liquefaction process; nevertheless, there are still a lot of issues needing to be addressed, for example, the complicated production procedure and Life Cycle Assessment (LCA). This work was expected to provide a fundamental data to simplify the production procedure in dependent on the analysis of thermal properties. The LCA process will be under consideration in the future works.

EXPERIMENTAL

Materials

Yaupon holly (*Ilex vomitoria*) (2.2 to 5.7 cm in diameter, 4.1 to 7.5 m in height) was collected at the Bob R. Idlewild Research Station (30°50'38.0"N 90°58'06.4"W) near

Clinton, LA, USA. After air drying, it was ground into 16- to 40-mesh and oven-dried at 105 °C until it reached a constant weight. The chemical composition of the Yaupon holly was as follows: α -cellulose (45.26%), hemicellulose (28.10%), Klason lignin (23.46%), alcohol-toluene extracts (4.01%), 1% sodium hydroxide (NaOH) solubility (27.53%), hot-water extracts (9.20%), and ash content (5.53%). The holocellulose, α -cellulose, lignin content, hot-water extracts, alcohol-toluene extractives, 1% NaOH solubility, and ash content of the raw material were determined in accordance with ASTM D1104-56 (1971), ASTM D1103-60 (1971), ASTM D1106-96 (1996), ASTM D1110-96 (1996), ASTM D1107-96 (1996), ASTM D1109-84 (2001), and ASTM D1102-84 (2001), respectively. The hemicellulose content was established as reported by Zhang *et al.* (2012).

Polymeric methylene diphenyl diisocyanate (pMDI) (brand name: Rubinate M) with an average functionality of 2.7, isocyanate group (NCO) content of 31.0%, and viscosity of 192 cps at 25 °C; glycerol-based polyol with a hydroxyl value of 238 mg KOH/g (brand name: Jeffol FX 31-240); and a catalyst, dimethylcyclohexylamine (brand name: JEFFCAT DMCHA), were all kindly supplied by Huntsman Polyurethanes (Woodlands, TX, USA). Dow Corning 193 (Dow Corning Corporation, Midland, MI, USA) and deionized water were used as a surfactant and a blowing agent, respectively. Glycerol, ethylene glycol (EG), methanol, and 98% sulfuric acid were purchased from VWR International (Radnor, PA, USA). All of the chemicals were used without further purification.

Methods

Microwave liquefaction

Liquefaction of Yaupon holly was performed in a Milestone laboratory microwave oven (Shelton, CT, USA) equipped with an ATC-400FO automatic fiber optic temperature control system. A typical loading included 2 g of Yaupon holly powder, 6 g of liquefaction solvent (glycerol:EG = 3:1), and 0.09 g of sulfuric acid. The mixed reactants were sealed in 100-mL Teflon reaction vessels with magnetic stirring bars. Eight vessels were simultaneously subjected in a single run. The output power of microwave energy was auto-adjusted based on temperature feedback from a sensor under the maximum power of 800 W. The sealed vessels were subjected to microwave irradiation. The reaction temperature was increased from room temperature to the desired temperatures (120 °C, 140 °C, 160 °C, 180 °C and 200 °C) within 5 min and then maintained for 5 min. An ice bath was applied to quench the reaction when the reaction was completed. After cooling down, the liquefaction products located in odd-numbered vessels (*i.e.*, 1, 3, 5, and 7) were dissolved in 150 mL of methanol with constant stirring for 4 h and filtered through Whatman No. 4 filter paper (GE Healthcare, Chicago, IL, USA) to separate the liquid and solid residue. The liquid portion was evaporated at 65 °C under vacuum to remove methanol. The solid residue that remained on the filter paper was oven-dried and weighed to calculate solid residue content as per Eq. 1. The liquefaction products sealed in even-numbered vessels (*i.e.*, 2, 4, 6, and 8) were completely transferred to a sample storage bottle.

$$\text{Solid residue content (\%)} = \frac{\text{Weight of residue}}{\text{Weight of raw material}} \times 100 \quad (1)$$

Acid and hydroxyl numbers of bio-polyols

The acid and hydroxyl numbers (AN) of bio-polyols were determined in accordance with Gao *et al.* 2010. The procedure to determine acid number was as follows: A mixture of 1 g bio-polyol sample and 20 mL dioxane-water solution (4/1, v/v) was titrated with 0.1 mol/L NaOH to end-point (pH 8.3). The blank titration was conducted using the same procedure. The acid number was calculated according to Eq. 2:

$$AN = \frac{C-D}{W} \cdot N \cdot 56.1 \quad (2)$$

The procedure to determine hydroxyl number was as follows: 1 g of bio-polyol and 10 mL of phthalic anhydride solution (dissolving 150 g phthalic anhydride in 900 mL of dioxane and 100 mL pyridine) were added into a 150-mL beaker. The beaker was sealed and placed into a boiling water bath for 20 min. After cooling down, 20 mL of dioxane-water solution (4/1, v/v) and 5 mL of water were added to the beaker and then titrated with 1 mol/L NaOH to pH 8.3. Blank titration was conducted using the same procedure. The hydroxyl number (HN) was calculated according to Eq. 3:

$$HN = \frac{B-S}{W} \cdot N \cdot 56.1 + AN \quad (3)$$

where *AN* and *HN* represent acid number and hydroxyl number (mg KOH/g), *B* and *D* are the volume of NaOH standard solution consumed in blank titration (mL), *C* and *S* are the volume of NaOH standard solution consumed in sample titration (mL), *W* is the sample weight (g), and *N* stands for the equivalent concentration of NaOH standard solution (mol/L). Three replicates were done to obtain the acid and hydroxyl numbers.

Scanning electron microscopy (SEM)

A scanning electron microscope (JSM-6110, JEOL Ltd., Tokyo, Japan) was used to examine the morphology of the solid residues using a 10 kV accelerating voltage. A high-efficiency Everhart-Thonley (E-T) detector was used to obtain images at a 12 mm working distance. Test samples were prepared for SEM inspection by coating them with gold using an EMS 550 X sputter coater (Electron Microscopy Science, Hatfield, PA, USA). Typical image of solid residues was selected from 3 sample replicates.

Preparation of polyurethane biofoams

Polyurethane foams were prepared by a one-step method. A mixture of 2.50 g liquefaction products (bio-polyol with or without residue), 2.5 g polyol (Jeffol FX 31-240), 0.20 g deionized water, 0.20 g catalyst (JEFFCAT DMCHA), and 0.20 g surfactant (Dow Corning 193) was thoroughly premixed in a 150-mL paper cup with a mechanical stirrer for 1 min. Afterwards, 11 g of pMDI was added to the mixture with stirring at 1500 rpm for 3 min. Neat foam and the biofoams without solid residues from reaction temperatures of 120 °C, 160 °C, and 200 °C were named as PU0, PU120, PU160, and PU200, respectively; the corresponding biofoams made from bio-polyols with solid residues were labeled as PU120R, PU160R, and PU200R. All of the PU foam samples were allowed to freely rise and cure at ambient conditions for two days before characterization.

FTIR analysis

The FTIR analysis was performed on a Nicolet Nexus 670 spectrometer (Madison Instruments, Middleton, WI, USA) equipped with a Thermo Nicolet Golden Gate MKII

Single Reflection ATR accessory equipped with a hybrid diamond/ZnSe single crystal (Brilliant Spectroscopy, PA, USA). A small quantity of sample powders was covered flatwise on the detection window. Each sample was analyzed in the range of resolution from 400 cm^{-1} to 4000 cm^{-1} with a spectral resolution of 4 cm^{-1} , and 32 scans were collected. Three replicates were used in this work.

The FTIR spectra of PU foams were baseline-flattened and normalized on the peak between 1595 cm^{-1} and 1600 cm^{-1} (phenyl band). Peak amplitude ratios were used for quantitative analysis. The HBI is the ratio of hydrogen-bonded carbonyl stretch (approximately 1708 cm^{-1}) to free carbonyl stretch (approximately 1730 cm^{-1}) in the urethane linkage. The EI is the ratio of aliphatic ether (C-O-C) stretch in the soft segment (approximately 1113 cm^{-1}) to the urethane ether (N-C-O-C) stretch in the hard segment (approximately 1068 cm^{-1}) (Tien and Wei 2001; Ebert *et al.* 2005; Zhang *et al.* 2013).

Thermogravimetric analysis (TGA)

The thermogravimetric analysis (TGA) was conducted with a thermal analyzer (model Q50 TGA; TA Instruments, New Castle, DE, USA) to obtain thermogravimetric data. Each sample of approximately 5 mg was conducted at $30\text{ }^{\circ}\text{C}$ to $800\text{ }^{\circ}\text{C}$ with a constant heating rate of $20\text{ }^{\circ}\text{C}/\text{min}$ under a flow of 40 mL/min of nitrogen atmosphere. Universal Analysis 2000 software from TA Instruments and ORIGIN 8.5 software were applied to analyze the obtained data. To verify the reproducibility of obtained mass loss curves, two sample runs were performed under the same experimental conditions. The approximate overlapping of two weight loss curves from two separate test runs was considered as reasonable; otherwise, another two runs were performed then to determine which one should be chosen.

RESULTS AND DISCUSSION

Characterization of Liquefaction

Figure 1 shows the variation of solid residue content with respect to the liquefaction temperature. Increasing the temperature from $120\text{ }^{\circ}\text{C}$ to $160\text{ }^{\circ}\text{C}$ resulted in a dramatic reduction in solid residue from 17.74% to 5.10%. In contrast, further increasing the temperature to $200\text{ }^{\circ}\text{C}$ resulted in a slight increase in the solid residue; it was somehow attributed to the re-condensation/repolymerization of decomposed wood components (Budijia *et al.* 2009).

As visible from the SEM images of the solid residue (Fig. 2(b)), the well-organized fiber bundles were collapsed at $120\text{ }^{\circ}\text{C}$. This result was ascribed to the rapid decomposition of hemicellulose and lignin, which are more susceptible to the liquefaction process than cellulose at low temperatures (Zhang *et al.* 2012). This was confirmed by the FTIR analysis of solid residue obtained from $120\text{ }^{\circ}\text{C}$ (Fig. 3). The characteristic IR absorbance bands of hemicellulose and lignin became weak after liquefaction at $120\text{ }^{\circ}\text{C}$, such as 1730 cm^{-1} (acetyl and uronic ester groups in hemicellulose), 1594 cm^{-1} (C=C skeletal vibration in aromatic rings), 1502 cm^{-1} (C=C skeletal vibration in aromatic rings), 1456 cm^{-1} (C-H bending in aromatic rings), and 1235 cm^{-1} (vibration of guaiacyl ring) (Poletto *et al.* 2012; Li *et al.* 2015).

The decompositions of hemicellulose and lignin, in turn, intensified the cellulose characteristic IR peaks, such as 1420 cm^{-1} (C-H₂ symmetric bending), 1322 cm^{-1} (C-H₂ rocking vibration), 1157 cm^{-1} (C-O-C asymmetric stretching), 1105 cm^{-1} (C-O stretching),

and 899 cm^{-1} (C-H deformation) (Chen *et al.* 2014; Li *et al.* 2015). The increase of methyl and/or methylene IR bands at 2928 cm^{-1} and 2850 cm^{-1} gave evidence of the breakdown of macromolecules in wood (Chen *et al.* 2014).

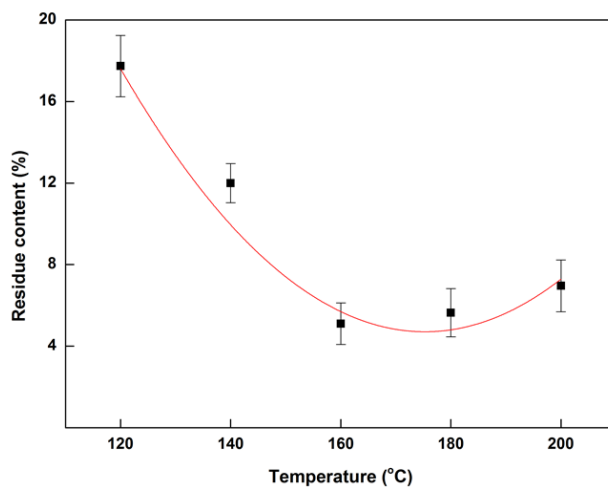


Fig. 1. Solid residue content with respect to reaction temperature (other conditions: solvent:solid = 3:1, H_2SO_4 : 1.5%, reaction time: 10 min)

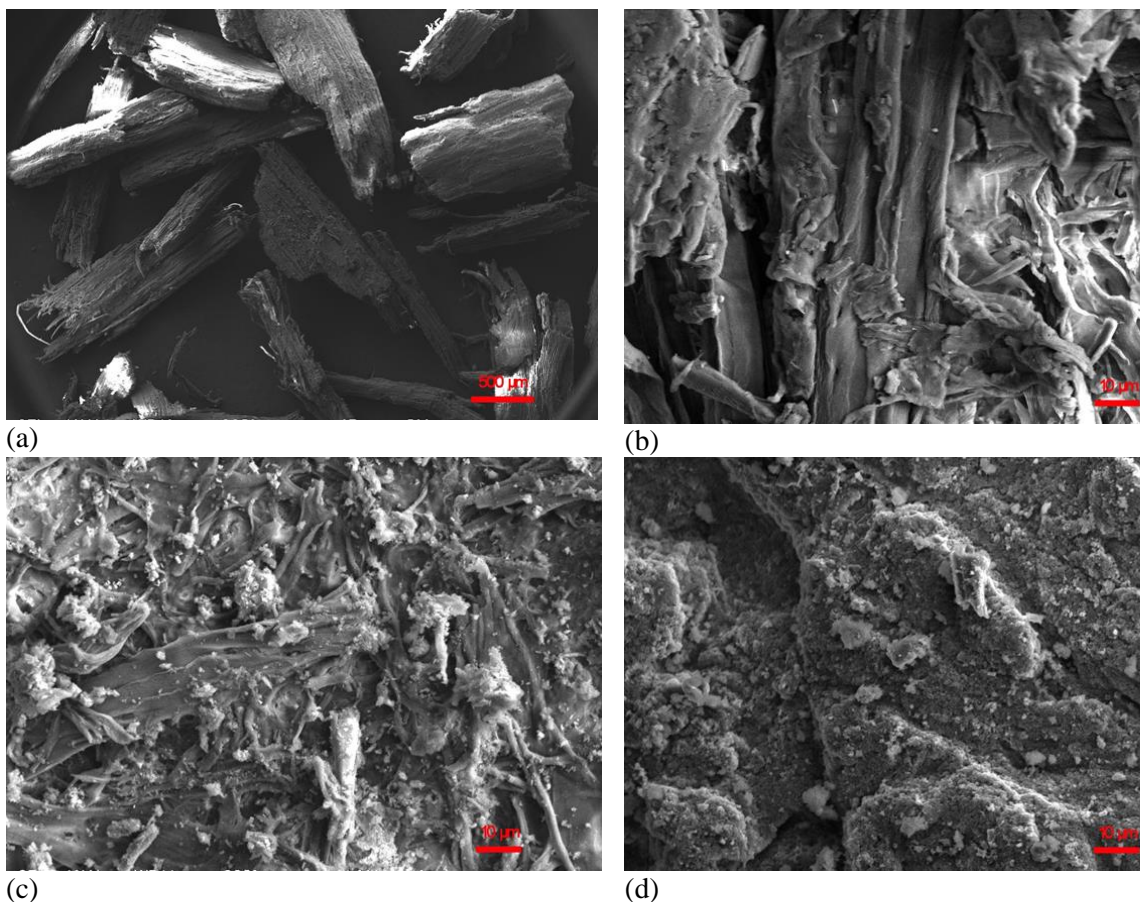


Fig. 2. SEM images of solid residue with respect to reaction temperature: (a) raw material, (b) $120\text{ }^\circ\text{C}$, (c) $160\text{ }^\circ\text{C}$, (d) $200\text{ }^\circ\text{C}$ (other conditions: solvent:solid = 3:1, H_2SO_4 : 1.5%, reaction time: 10 min)

Figure 2(c) shows that the cellulose bundles were broken down to small irregular fragments as the temperature increased to 160 °C. Spherical granular substances were also observed on the solid surface, suggesting repolymerization of liquefied fragments, which contributes to the increase of solid residue. The decomposition of the main chemical components of wood contributed to increased hydroxyl IR absorbance intensity at 3340 cm^{-1} . However, it became weak at 160 °C, due to the repolymerization process. When the temperature was further increased to 200 °C, most of the cellulosic structures disappeared due to the decomposition of cellulose, which was confirmed by the FTIR analysis.

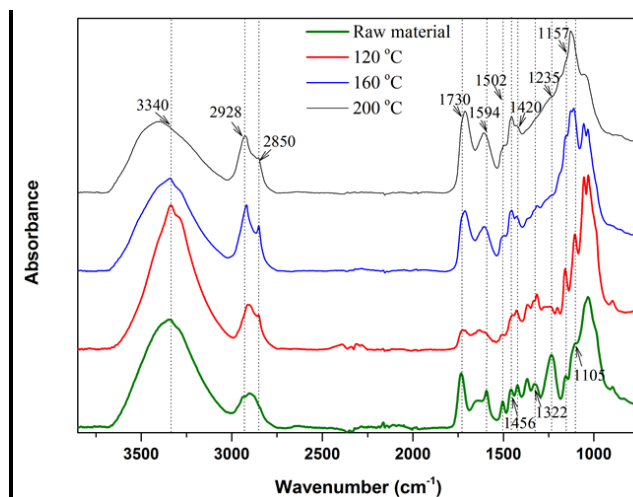


Fig. 3. FTIR spectra of raw material and solid residues with respect to reaction temperature (other conditions: solvent:solid = 3:1, H_2SO_4 : 1.5%, reaction time: 10 min)

For the bio-polyol, the acid and hydroxyl numbers are shown in Table 1. The acid number of bio-polyol decreased from 5.58 mg KOH/g to 1.10 mg KOH/g, and the hydroxyl number decreased from 379.4 mg KOH/g to 344.1 mg KOH/g as the temperature increased from 120 °C to 200 °C. These tendencies were in agreement with the results reported by Hu and Li (2014). The decrease in acid number was attributable to the consumption of acidic compounds involved in esterification, transesterification, and etherification reactions (Lee *et al.* 2016). The decreasing hydroxyl number of bio-polyol was ascribed to dehydration, condensation, and thermal oxidation reactions during liquefaction (Lee *et al.* 2000). Accordingly, the liquefaction products, including solid residue and bio-polyol, changed with reaction temperature, suggesting that the thermal stability of biofoams made from the liquefaction products may vary with temperature.

Table 1. Acid Number and Hydroxyl Number of Bio-Polyols with Respect to Reaction Temperature

Temperature (°C)	Acid Number (mg KOH/g)	Hydroxyl Number (mg KOH/g)
120	5.58 ± 0.71	379.36 ± 5.18
160	1.12 ± 0.47	374.37 ± 7.92
200	1.10 ± 0.32	344.14 ± 8.51

Thermal Stability of Biofoams Without Solid Residue

The TG and DTG curves of neat foam and biofoams without solid residue as a function of liquefaction temperature are shown in Fig. 4. Their thermal degradation features are summarized in Table 2. All biofoams showed TGA curves with similar shapes, suggesting similar thermal degradation behaviors. The weight loss up to 140 °C was due to the evaporation of moisture content and the release of thermally unstable EG (Fig. 5 and Table 3). The onset degradation temperature (5% weight loss, T_{onset}) of biofoams without solid residue was in the range of 256.51 °C to 263.00 °C, which was slightly higher than that of the neat foam (Table 2). The onset degradation temperature was also slightly higher than for other bio-based PU foams made from wood bark and corn stover (Zhao *et al.* 2012; Hu and Li 2014). Moreover, all the maximum degradation temperatures (T_{max}) of biofoams were higher than those of the neat foam. This result indicated that the substitution of petro-based polyol with bio-polyol from liquefaction increased the thermal stability of PU foam, because the bio-polyol with multi hydroxyl group components (C5 and C5 sugars) could enhance the urethane linkage density (Huang *et al.* 2018). The first degradation stage at around 325 °C could be assigned to the unstable urethane bonds (Hablott *et al.* 2008; Hakim *et al.* 2011), and it also could be partially ascribed to the degradation of glycerol, as shown in Table 3. The second stage at approximately 369 °C corresponded to the degradation of polyol, as shown in Fig. 5 and Table 3. The third degradation stage at 426 °C was only observed for PU120. This unique peak could be attributed to the degradation of lignin components in bio-polyol introduced by liquefaction (Huang *et al.* 2017). The fourth stage at approximately 500 °C was ascribed to the degradation of pMDI, which was confirmed in Fig. 5 and Table 3. Moreover, it also corresponded to the degradation of lignin and other more difficult-to-break parts formed in previous stages (Ertaş *et al.* 2014). The char yields of biofoams were higher than the corresponding values for neat foam; this result was due to the introduction of ash components from wood.

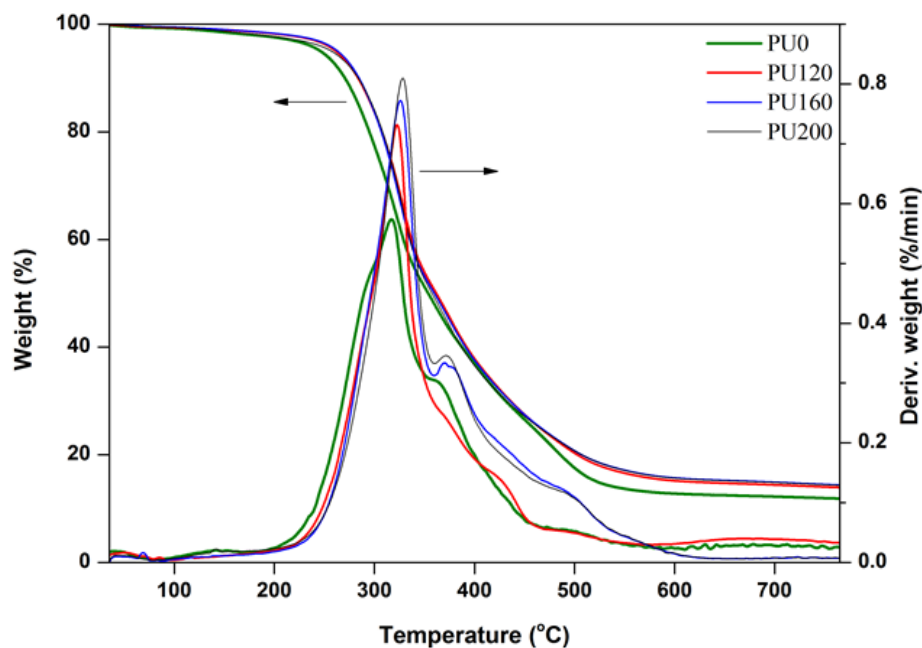
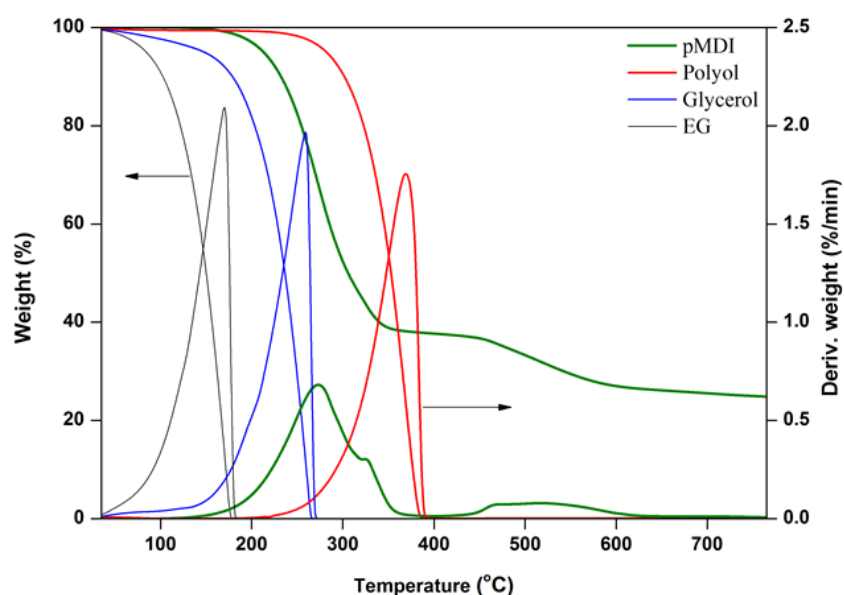


Fig. 4. TG and DTG curves of biofoams made from bio-polyols without solid residue

Table 2. Thermal Degradation Features of Biofoams

Foam ID	T_{onset} (°C)	T_{max} (°C)				Char Yield (%)
		Stage 1	Stage 2	Stage 3	Stage 4	
PU0	251.00	317.24	367.94	–	495.87	12.00
PU120	256.51	322.76	371.29	426.22	498.24	14.49
PU160	263.00	326.10	369.92	–	496.98	14.42
PU200	256.84	328.43	371.59	–	501.56	14.35
PU120R	259.67	331.43	369.25	–	498.24	14.52
PU160R	265.84	326.93	373.94	–	499.34	14.80
PU200R	258.38	329.10	371.42	–	502.66	14.74

**Fig. 5.** TG and DTG curves of pMDI, polyol, glycerol, and ethylene glycol (EG)**Table 3.** Thermal Degradation Features of pMDI, Polyol, Glycerol, and EG

Chemical	T_{onset} (°C)	T_{max} (°C)		Char Yield (%)
		Stage 1	Stage 2	
pMDI	212.88	273.11	516.68	24.86
Polyol	281.93	368.85	–	0.19
Glycerol	147.48	259.29	–	0.03
EG	84.15	169.94	–	0.11

When the liquefaction temperature was increased from 120 °C to 200 °C, the degradation temperature of urethane bonds was gradually increased from 322.8 °C to 328.4 °C. Notably, excessive isocyanate did not increase the formation urethane bond density, which was indicated from the FTIR analysis of PU foams. The characteristic urethane bond at around 3330 cm^{-1} (N-H stretching) decreased with the increase of liquefaction temperature (Fig. 6(b)). This result indicated that the urethane bond density decreased with increasing temperature. Nevertheless, the excessive free isocyanate (pMDI) could contribute to forming a higher crosslink density, and thus increase the thermal stability of biofoams (Zhao *et al.* 2012).

Figure 6(a) presents typical IR spectra of PU foams. For instance, the presence of urethane bonds could be observed from peaks of 3330 cm^{-1} (N-H), 1730 cm^{-1} (C=O), 1310 cm^{-1} (N-H), 1218 cm^{-1} (C-N), 1114 cm^{-1} (C-O-C), and 1070 cm^{-1} (N-C-O-C) (Tien and Wei 2001; Zhao *et al.* 2012; Ugarte *et al.* 2017). The bands at 1507 cm^{-1} and 1596 cm^{-1} were derived from aromatics of pMDI (Li *et al.* 2013). The peaks at 2915 cm^{-1} and 1410 cm^{-1} were attributed to methylene and the aromatic rings, respectively (Gu *et al.* 2012; Zhao *et al.* 2012). An excessive amount of pMDI at 2275 cm^{-1} was used deliberately to ensure that hydroxyl components could completely react with NCO groups.

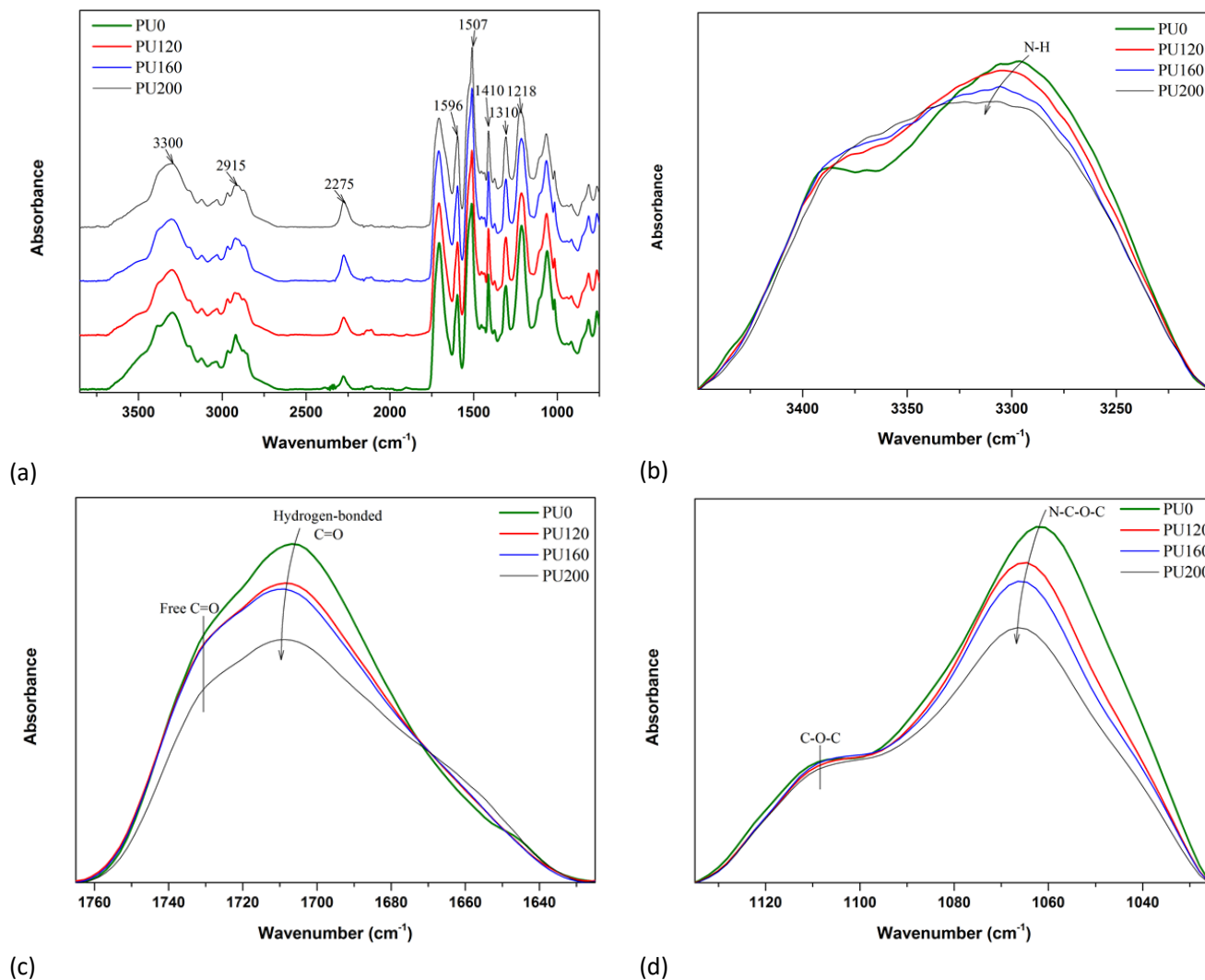


Fig. 6. FTIR spectra of biofoams made from bio-polyols without solid residue

The intensity of hydrogen-bonded carbonyl of biofoams decreased more than that of free carbonyl compared to the neat foam (Fig. 6(c)), which suggested that fewer urethane bonds were hydrogen bonded in biofoams. It was further evidenced from Table 4 that the carbonyl HBI values for biofoams were lower than the corresponding value for neat foam. The urethane ethers' (N-C-O-C) stretch in hard segments of biofoams and the EI values for biofoams were lower than those for neat foam (Fig. 6(d)), indicating that the bio-polyol undermined the formation of hard segments.

Increasing the liquefaction temperature from 120 °C to 160 °C, the intensity of hydrogen-bonded carbonyl of biofoams slightly decreased, while the free carbonyl remained stable, resulting in the HBI decreasing from 1.26 to 1.24. Further increasing the temperature to 200 °C, both hydrogen-bonded and free carbonyl rapidly decreased. The hydroxyl number of bio-polyol remarkably decreased as the temperature was increased from 160 °C to 200 °C (Table 1), which led to the decrease of urethane bond density in PU200. Therefore, it was reasonable that the intensities of hydrogen-bonded and free carbonyl of biofoams decreased at 200 °C. Figure 6(d) shows that the urethane ethers' (N-C-O-C) stretch in the hard segments of biofoams rapidly decreased with increasing liquefaction temperature and shifted to a higher wavenumber, while the aliphatic ether (C-O-C) was not remarkably affected by the change of liquefaction temperature, suggesting that fewer hard segments were formed with increasing liquefaction temperature. This result was attributed to fewer urethane bonds (hard segments) being formed due to the decrease of hydroxyl number with temperature. Moreover, the increasing EI of biofoams further demonstrated this result, as shown in Table 4.

Table 4. Carbonyl HBI and EI of Biofoams

Foam ID	HBI	EI
PU0	1.37	0.34
PU120	1.26	0.37
PU160	1.24	0.40
PU200	1.26	0.45
PU120R	1.25	0.44
PU160R	1.26	0.45
PU200R	1.25	0.48

Thermal Stability of Biofoams with Solid Residue

The thermal stability of biofoams with solid residue is shown in Fig. 7. The TGA curves of biofoams with solid residue were similar to those of biofoams without solid residue.

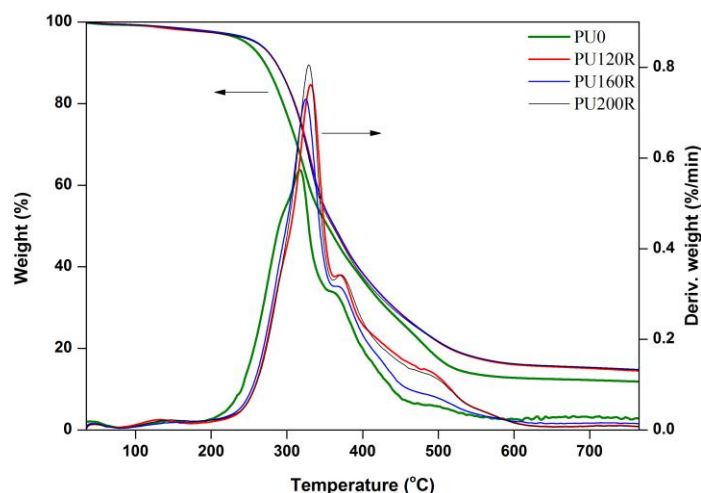


Fig. 7. TG and DTG curves of biofoams made from bio-polyols with solid residue

Notably, the onset temperature, maximum degradation temperature of the first stage, and char yield of biofoams with solid residue were greater than those of biofoams without residue (Table 2). The increased onset temperature was probably due to the decrease of thermally unstable glycerol (which is unstable at approximately 260 °C, as shown in Table 3), as the presence of solid residue in bio-polyol led to a decrease in the liquid portion. The increased maximum degradation temperature at the first stage probably was due to an increase of crosslink density. The increase of char yield was ascribed to the introduction of ash components in solid residue.

The FTIR analysis of biofoams with solid residue also presented typical PU foam IR absorbance characteristics (Fig. 8(a)). The characteristic urethane bonds (N-H stretching) of biofoams with solid residue at around 3330 cm^{-1} decreased with increasing liquefaction temperature (Fig. 8(b)), a similar behavior to biofoams without solid residue.

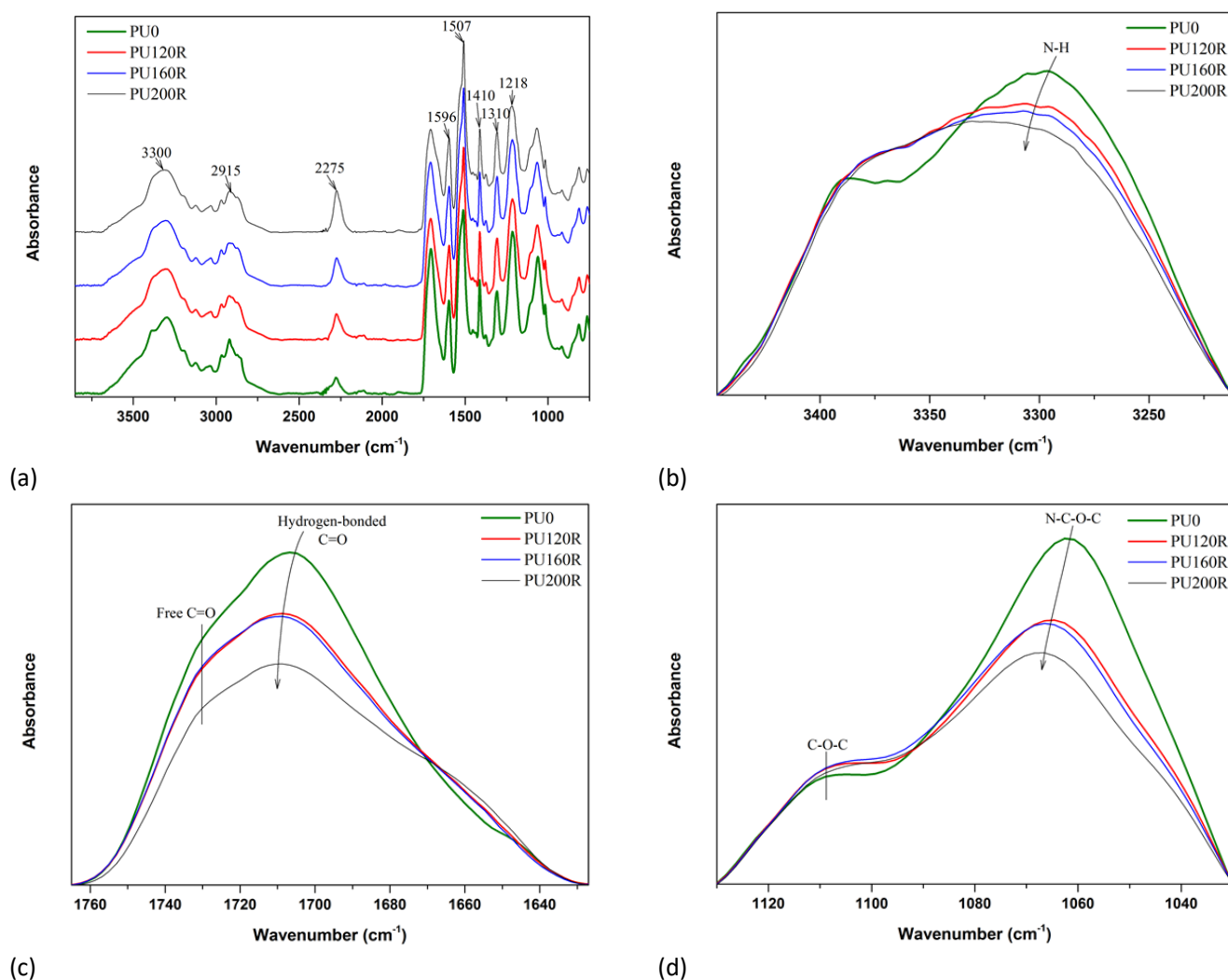


Fig. 8. FTIR spectra of biofoams made from bio-polyols with solid residue

Increasing liquefaction temperature from 120 °C to 160 °C did not remarkably affect the IR intensities of free and hydrogen-bonded carbonyls in biofoams with solid residue. However, both the free and hydrogen-bonded carbonyls decreased remarkably as the temperature increased to 200 °C. As visible from Table 4, there was no clear

difference in carbonyl HBI between the biofoams with and without solid residue. In general, the variation of HBI was related to the mobility of PU molecular chains, as high mobility could promote the urethane bonds to form hydrogen bonds (Tien and Wei 2001). Therefore, the solid residue did not remarkably affect the mobility of the urethane bonds in the resulting biofoams. The EI of biofoams increased with increasing liquefaction temperature. This result was ascribed to the decrease of the intensity of urethane ethers' (N-C-O-C) stretch in hard segments (Fig. 8(d)). Apart from this, the EI values of biofoams with solid residue were higher than those of biofoams without solid residue, which suggested that the presence of solid residue undermined the formation of hard segments in biofoams.

CONCLUSIONS

1. Solid residue content rapidly decreased when liquefaction temperature increased from 120 °C to 160 °C and then slightly increased when further increasing temperature to 200 °C.
2. The thermal stability of biofoams was greater than that of petro-based neat foam, indicating that the substitution of petro-based polyol with liquefaction bio-polyol had a positive effect on the thermal stability of PU foams.
3. With increasing liquefaction temperature, the urethane bond density of biofoams decreased due to the decrease of hydroxyl number.
4. The presence of solid residue enhanced the thermal stability of biofoams, as indicated from the increased onset degradation temperature, and the solid residue undermined the formation of hard segments (urethane bond).

ACKNOWLEDGMENTS

This work was partially supported by the Fundamental Research Funds for the Central Non-profit Research Institution of Chinese Academy of Forestry (CAFYBB2018MA006) and the USDA Forest Service 2015 Wood Innovations Funding Opportunity program, Agreement 15-DG-11083150-054; and the USDA National Institute of Food and Agriculture, McIntire-Stennis project 94118. The authors also appreciate the financial support of the China Scholarship Council, the National Natural Science Foundation of China (31700578), and the Open Fund of Guangxi Key Laboratory of Clean Pulp & Papermaking and Pollution Control, Nanning 530004, China (KF201722).

REFERENCES CITED

- ASTM D1102-84 (2001). "Standard test method for ash solubility of wood," ASTM International, West Conshohocken, PA.
- ASTM D1103-60 (1971). "Standard test method for alpha-cellulose in wood," ASTM International, West Conshohocken, PA.

- ASTM D1104-56 (1971). "Standard test method for holocellulose in wood," ASTM International, West Conshohocken, PA.
- ASTM D1106-96 (1996). "Standard test method for acid-insoluble lignin in wood," ASTM International, West Conshohocken, PA.
- ASTM D1107-96 (1996). "Standard test method for ethanol-toluene solubility of wood," ASTM International, West Conshohocken, PA.
- ASTM D1109-84 (2001). "Standard test method of 1% sodium hydroxide solubility of wood," ASTM International, West Conshohocken, PA.
- ASTM D1110-96 (1996). "Standard test for water solubility of wood," ASTM International, West Conshohocken, PA.
- Budija, F., Tavzes, Č., Zupančič-Kralj., and Petrič, M. (2009). "Self-crosslinking and formation ability of liquefied black polar," *Bioresource Technology* 100(13), 3316-3323. DOI: 10.1016/j.biortech.2009.02.004
- Chen, C., Luo, J., Qin, W., and Tong, Z. (2014). "Elemental analysis, chemical composition, cellulose crystallinity, and FT-IR spectra of *Toona sinensis* wood," *Monatshefte für Chemie - Chemical Monthly* 145(1), 175-185. DOI: 10.1007/s00706-013-1077-5
- Chen, F., and Lu, Z. (2009). "Liquefaction of wheat straw and preparation of rigid polyurethane foam from the liquefaction products," *Journal of Applied Polymer Science* 111(1), 508-516. DOI: 10.1002/app.29107
- Ebert, M., Ward, B., Anderson, J., McVenes, R., and Stokes, K. (2005). "In vivo biostability of polyether polyurethanes with polyethylene oxide surface-modifying end groups; resistance to biologic oxidation and stress cracking," *Journal of Biomedical Materials Research Part A* 75A(1), 175-184. DOI: 10.1002/jbm.a.30396
- Ertas, M., Fidan, M. S., and Alma, M. H. (2014). "Preparation and characterization of biodegradable rigid polyurethane foams from the liquefied eucalyptus and pine woods," *Wood Research* 59(1), 97-108.
- Esteves, B., Dulyanska, Y., Costa, C., Ferreira, J. V., Domingos, I., Pereira, H., de Lemos, L. T., and Cruz-Lopes, L. V. (2017). "Cork liquefaction for polyurethane foam production," *BioResources* 12(2), 2339-2353. DOI: 10.15376/biores.12.2.2339-2353
- Gama, N. V., Soares, B., Freire, C. S. R., Silva, R., Neto, C. P., Barros-Timmons, A., and Ferreira, A. (2015). "Bio-based polyurethane foams toward applications beyond thermal insulation," *Materials & Design* 76, 77-85. DOI: 10.1016/j.matdes.2015.03.032
- Gao, L.-L., Liu, Y.-H., Lei, H., Peng, H., and Ruan, R. (2010). "Preparation of semirigid polyurethane foam with liquefied bamboo residues," *Journal of Applied Polymer Science* 116(3), 1694-1699. DOI: 10.1002/app.31556
- Cheumani-Yona, A. M., Budija, F., Hrastnik, D., Kutnar, A., Palič, M., Pori, P., Tavzes, Č., and Petrič, M. (2015). "Preparation of two-component polyurethane coating from bleached liquefied wood," *BioResources* 10(2), 3347-3363. DOI: 10.15376/biores.10.2.3347-3363
- Cheumani-Yona, A. M., Budija, F., Kričej, B., Kutnar, A., Palič, M., Pori, P., Tavzes, Č., and Petrič, M. (2014). "Production of biomaterials from cork: Liquefaction in polyhydric alcohols at moderate temperatures," *Industrial Crops and Products* 54: 296-301. DOI: 10.1016/j.indcrop.2014.01.027
- Gu, R., Konar, S., and Sain, M. (2012). "Preparation and characterization of sustainable polyurethane foams from soybean oils," *Journal of the American Oil Chemists' Society* 89(11), 2103-2111. DOI: 10.1007/s11746-012-2109-8

- Hablot, E., Zheng, D., Bouquey, M., and Avérous, L. (2008). "Polyurethanes based on castor oil: Kinetics, chemical, mechanical and thermal properties," *Macromolecular Materials and Engineering* 293(11), 922-929. DOI: 10.1002/mame.200800185
- Hakim, A. A. A., Nassar, M., Emam, A., and Sultan, M. (2011). "Preparation and characterization of rigid polyurethane foam prepared from sugar-cane bagasse polyol," *Materials Chemistry and Physics* 129(1-2), 301-307. DOI: 10.1016/j.matchemphys.2011.04.008
- Hu, S., and Li, Y. (2014). "Two-step sequential liquefaction of lignocellulosic biomass by crude glycerol for the production of polyols and polyurethane foams," *Bioresour Technol* 161, 410-415. DOI: 10.1016/j.biortech.2014.03.072
- Huang, X.-Y., de Hoop, C. F., Xie, J.-L., Wu, Q.-L., Boldor, D., and Qi, J.-Q. (2018). "High bio-content polyurethane (PU) foam made from bio-polyol and cellulose nanocrystals (CNCs) via microwave liquefaction," *Materials & Design* 138, 11-20. DOI: 10.1016/j.matdes.2017.10.058
- Huang, X.-Y., Li, F., Xie, J.-L., de Hoop, C. F., Hse, C.-Y., Qi, J.-Q., and Xiao, H. (2017). "Microwave-assisted liquefaction of rape straw for the production of bio-oils," *BioResources* 12(1), 1968-1981. DOI: 10.15376/biores.12.1.1968-1981
- Kumar, A., Vlach, T., Ryparovà, P., Škapin, A. S., Kovač, J., Adamopoulos, S., Hajek, P., and Petrič, M. (2017). "Influence of liquefied wood polyol on the physical-mechanical and thermal properties of epoxy based polymer," *Polymer Testing* 64, 207-216. DOI: 10.1016/j.polymertesting.2017.10.010
- Lee, J.-H., Lee, J. H., Kim, D.-K., Park, C.-H., Yu, J.-H., and Lee, E. Y. (2016). "Crude glycerol-mediated liquefaction of empty fruit bunches saccharification residues for preparation of biopolyurethane," *Journal of Industrial and Engineering Chemistry* 34, 157-164. DOI: 10.1016/j.jiec.2015.11.007
- Lee, S.-H., Teramoto, Y., and Shiraishi, N. (2002). "Biodegradable polyurethane foam liquefied waste paper and its thermal stability, biodegradability, and genotoxicity," *Journal of Applied Polymer Science* 83(7), 1482-1489. DOI: 10.1002/app.10039
- Lee, S.-H., Yoshioka, M., and Shiraishi, N. (2000). "Liquefaction of corn bran (CB) in the presence of alcohols and preparation of polyurethane foam from its liquefied polyol," *Journal of Applied Polymer Science* 78(2), 319-325. DOI: 10.1002/1097-4628(20001010)78:2<319::AID-APP120>3.3.CO;2-Q
- Li, G., Hse, C., and Qin, T. (2015). "Wood liquefaction with phenol by microwave heating and FTIR evaluation," *Journal of Forestry Research* 26(4), 1043-1048. DOI: 10.1007/s11676-015-0114-0
- Li, S., Li, C., Li, C., Yan, M., Wu, Y., Cao, J., and He, S. (2013). "Fabrication of nanocrystalline cellulose with phosphoric acid and its full application in a modified polyurethane foam," *Polymer Degradation and Stability* 98(9), 1940-1944. DOI: 10.1016/j.polymdegradstab.2013.06.017
- Liang, L., Mao, Z., Li, Y., Wan, C., Wang, T., Zhang, L., and Zhang, L. (2006). "Liquefaction of crop residues for polyol production," *BioResources* 1(2), 248-256. DOI: 10.15376/biores.1.2.248-256
- Liu, H.-M., Xie, X.-A., Feng, B., and Sun, R.-C. (2011). "Effect of catalysts on 5-lump distribution of cornstalk liquefaction in sub-critical ethanol," *BioResources* 6(3), 2592-2604. DOI: 10.15376/biores.6.3.2592-2604
- Poletto, M., Zattera, A. J., and Santana, R. M. C. (2012). "Structural differences between wood species: Evidence from chemical composition, FTIR spectroscopy, and thermogravimetric analysis," *Journal of Applied Polymer Science* 126(S1), E337-

E344. DOI: 10.1002/app.36991

- Tien, Y. I., and Wei, K. H. (2001). "Hydrogen bonding and mechanical properties in segmented montmorillonite/polyurethane nanocomposites of different hard segment ratios," *Polymer* 42(7), 3213-3221. DOI: 10.1016/S0032-3861(00)00729-1
- Ugarte, L., Santamaria-Echart, A., Mastel, S., Autore, M., Hillenbrand, R., Corcuera, M. A., and Eceiza, A. (2017). "An alternative approach for the incorporation of cellulose nanocrystals in flexible polyurethane foams based on renewably sourced polyols," *Industrial Crops and Products* 95, 564-573. DOI: 10.1016/j.indcrop.2016.11.011
- Xue, B.-L., Wen, J.-L., and Sun, R.-C. (2015). "Producing lignin-based polyols through microwave-assisted liquefaction for rigid polyurethane foam production," *Materials* 8(2), 586-599. DOI: 10.3390/ma8020586
- Yan, Y., Pang, H., Yang, X., Zhang, R., and Liao, B. (2008). "Preparation and characterization of water-blown polyurethane foams from liquefied cornstalk polyol," *Journal of Applied Polymer Science* 110(2), 1099-1111. DOI: 10.1002/app.28692
- Zhang, C., and Kessler, M. R. (2015). "Bio-based polyurethane foam made from compatible blends of vegetable-oil-based polyol and petroleum-based polyol," *ACS Sustainable Chemistry & Engineering* 3(4), 743-749. DOI: 10.1021/acssuschemeng.5b00049
- Zhang, H., Pang, H., Shi, J., Fu, T., and Liao, B. (2012). "Investigation of liquefied wood residues based on cellulose, hemicellulose, and lignin," *Journal of Applied Polymer Science* 123(2), 850-856. DOI: 10.1002/app.34521
- Zhang, H., Pang, H., Zhang, L., Chen, X., and Liao, B. (2013). "Biodegradability of polyurethane foam from liquefied wood based polyols," *Journal of Polymers and the Environment* 21(2), 329-334. DOI: 10.1007/s10924-012-0542-2
- Zhao, Y., Yan, N., and Feng, M. (2012). "Polyurethane foams derived from liquefied mountain pine beetle-infested barks," *Journal of Applied Polymer Science* 123(5), 2849-2858. DOI: 10.1002/app.34806

Article submitted: January 11, 2018; Peer review completed: February 26, 2018; Revised version received and accepted March 12, 2018; Published: March 15, 2018.

DOI: 10.15376/biores.13.2.3346-3361